Vol. 45, No. 4 (2023) 618-633, DOI: 10.24874/ti.1441.01.23.04

Tribology in Industry

www.tribology.rs

RESEARCH

Analysis and Optimization of Nanolubricated Journal Bearing under Thermoelasto-Hydrodynamic Lubrication Considering Cavitation Effect

Basim A. Abass[a], Saba Y. Ahmed[a], Zainab H. Kadhim[b,*]

[a]*University of Babylon, College of Engineering, Mechanical Engineering Department, Iraq,*
[b]*Al-Amarah University College, Mechanical Engineering Department, Iraq.*

Keywords:

Journal bearing
Nano-lubrication
CFD analysis
Elastic deformation
Thermal effect
Cavitation effect
Optimization

* Corresponding author:

Zainab H. Kadhim
E-mail:
zaynab.hafid@alamarahuc.edu.iq

Received: 24 January 2023
Revised: 13 March 2023
Accepted: 9 April 2023

A B S T R A C T

This work deals with the effect of the cavitation and the elastic deformation on the steady-state thermal performance of plain journal bearing using CFD-FSI technique. As a case study, a bearing lubricated with SAE40W oil dispersed with TiO_2 nanoparticles was extensively analyzed. The hydrodynamic pressure, oil film temperature, and the other bearing parameters have been calculated. The nanoparticles volume fractions, journal speeds, and eccentricity ratios have been considered. Krieger Dougherty model was implemented with the Vogel- Barus exponential viscosity to include the effects of the oil temperature and TiO_2 nanoparticles volume fraction on the lubricant viscosity. The cavitation effect was implemented using Zwart-Gerber-Belamari model. The optimum journal position, the attitude angle, and the load have been obtained using Multi-Objective Genetic Algorithm. The mathematical model was successfully verified with the pressure and the total deformation published by Dhande with 4% and 2% deviation between the results respectively. The film temperature of the present work was compared to that obtained numerically by Li et al and experimentally by Ferron and Boncompain with 2% maximum deviation between the results. An enhancement in the load-carrying capacity of the bearing with a little growth in oil film temperature were obtained when using TiO_2 nano lubricant.

1. INTRODUCTION

Journal bearing is a machine element used to support high speed and high load rotors. It suffers from the rise of the oil film temperature and cavitation during the work under such circumstances which affects the bearing performance. For a more realistic analysis, it is important to take the oil temperature and cavitation effects on the bearing performance into consideration. It was also noticed that increased severeness of load and speed in modern machines obliged improved solutions to enhance the performance of the supporting bearings. Hence, in addition to the new designs of the bearing configurations, importance is given to improving the properties of the oil used. It was observed that the residence of small particles in nanoscales improves the lubricant properties. Nair et al. [1] and Kalakada et al. [2] presented static performance characteristics of journal bearing lubricated with CuO, CeO_2, and Al_2O_3 nano-lubricants. It was observed that the addit-ion of such nanoparticles causes an enhancement of the base oil viscosity which in turn affects the bearing performance characteristics. Krieger Dougherty viscosity model was found to be the more realistic model used by different workers to include the lubricant thermo-viscous effect of the nano-lubricants on static characteristics of the journal bearing [3-6]. It was observed that the load carried by the bearing enhances when it was lubricated with this type of lubricant. Kumar and Kakoty [7] and [8] studied the static and dynamic characteristics of two- and three-lobe journal bearings operating with TiO_2 nano-lubricant using finite difference technique with Krieger Dougherty's model to assess the lubricant viscosity. It has been noticed that the bearing load, the flow coefficient, and the friction variable were enhanced in comparison with that lubricated with pure oil. Suryawanshi and Pattiwar [9] presented a comparative analysis for the performance of plain and elliptical journal bearings operating with industrial lubricant blended with TiO_2 nanoparticles and different journal speeds. It was observed that the elliptical bearing performance improves over the plain journal bearing operating under the same circumstances. Ramaganesh et al. [10] analyzed the performance of nano-lubricated journal bearing using the finite element method using COMSOL software. The suitability of the mathematical model to find the generated oil film pressure was clarified experimentally. Dhanola and Garg [11] studied the thermal behavior of the journal bearing lubricated with bio-based lubricant blended with TiO_2 nanoparticles using the adiabatic assumption with finite difference solution. An enhancement of the oil film pressure, the load carried by the bearing, and the traction force was obtained as a result of blending the nanoparticles in the base oil. Khan et al. [12] performed finite difference analysis of a cylindrical journal bearing lubricated with non-Newtonian nano-lubricant considering the bearing elasticity. The lubricant viscosity was calculated by implementing the Krieger Dougherty model with the power-law model. It has been demonstrated that the load-carrying capacity, the maximum pressure, and the friction force increased when using such lubricant. However, a significant effect of elastic deform-ation on the bearing performance was observed. Parthasarathy et al. [13] show that the optimum frictional coefficient of the journal bearing lubricated with nano-lubricant can be effectively estimated using the Fuzzy logic technique. Shantanu Salunke and Mahesh Gaikwad [14] show that the bearing performance character-ristics were enhanced when the bearing was lubricated with oil blended with CuO and Boron Nitride nanoparticles. Dang et al. [15] indicated that the load carried by a journal bearing enhances with small rise in oil film temperature when it was lubricated with oil degraded with CuO and TiO_2 nanoparticles. Krieger Dougherty model was used to evaluate the nano lubricants' viscosity. Gundarneeya and Vakharia [16] inve-stigated the performance of plain journal bearing lubricated with synthetic oil blended with TiO_2, Al_2O_3, and CuO nanoparticles using the conventional Reynolds equation technique. The results obtained indicated an enhancement in the load carried by the bearing when it was lubricated with such nano lubricants compared with that lubricated with pure oil. Different studies show that the CFD with fluid-structure interaction technique seems to be one of the most promising possibilities for theoretical analysis of lubrication problems considering the effects of different parameters. Liu et al. [17] used the CFD technique to study the elastohydrodynamic lubrication of a complex rotor system consid-ering the cavitation effect. The obtained results show that the journal center position was considerably affected by the elastic deformation of the bearing material. Benasciutti et al. [18] analyzed the performance of hydrodynamic radial journal bearing considering the effects of the oil film temperature and the shaft and the housing elastic deformations using finite element method. The obtained results show the great influence of the elastic deformation of the bearing components on the oil pressure distribution. Wodtke et al. [19] analyzed the steady-state performance of tilted pad thrust journal bearing using the CFD-FSI technique. Chauhan et al. [20] carried out a thermo-hydrodynamic analysis using the CFD approach to study circular journal bearing performance parameters. It has been noticed that the oil film temperature increases as a result of considering the variation of the oil viscosity. Zhang et al. [21] studied the effects of thermal and elastic deformations on lubricating properties of journal bearing considering surface roughness, variable viscosity, and cavitation effects using the CFD-FSI technique. It was noticed that the load-carrying capacity and the maximum oil film pressure decreased drastically when the combined thermal and elastic deformation was considered in comparison with the elastic deformation only. Chen et al. [22] investigated the effect of the oil groove location and lubrication performance of journal bearing in the high-speed and heavy-load system using CFD-FSI technique. Kyrkou and Nikolakopoulos [23] performed a thermoshydrodynamic analysis of a journal bearing lubricated with synthetic and environmentally friend oils using CFD technique. The present work includes a numerical test for the effect of an experimentally characterized nano-lubricant incorporated SAE40W oil blended with TiO_2 nanoparticles [24] on the performance of journal bearing considering the effects of the elastic deformation of the bearing material and the cavitation using CFD-FSI technique which is a useful tool for investigating the hydrodynamic and elastohydrodynamic lubrications of a rotor–bearing system. Also, the design of experiment, response surface analysis and the optimization technique were used to define the shaft equilibrium position.

2. MATHEMATICAL MODEL

2.1 Bearing geometry

The analysis of the present work was implemented considering a journal-bearing geometry illustrated in Fig. 1. The bearing geometrical and operation characteristics in addition to the physical properties of the lubricant used are illustrated in table (1).

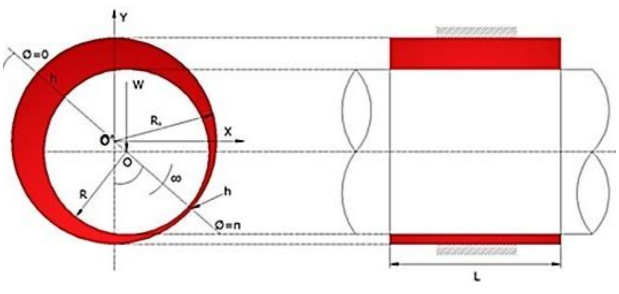

Fig. 1. Bearing geometry.

Table 1. Geometrical and physical properties.

Parameter	Parameter
L/D=0.5	β=0.032°C^{-1}
r_s=24.95mm	ρ_m=875kg/m^3
r_i=25mm	$C_{Poil} = 2000 J/kg.^oC$
r_o=30mm	k_{oil}=0.13W/m.°C
ε[0.1-0.9]	P_V=29185Pa
ϕ=49°	φ=0-3%
N=[2000-4000 rpm]	$\mu_i = 0.078[N.s/m^2$
T_i=40°C	C=0.05[mm]

2.2 Governing equations

Continuity Equation [22]

$$\frac{\partial}{\partial t}(\rho_f) + \nabla.(\rho_f \vec{v}) = 0 \quad (1)$$

ρ_f is the fluid density which assumed to be constant in the present work.

$\vec{v}$ is the fluid vector velocity

Momentum Equation

The bearing oil film pressure distribution can be evaluated by solving the Navier-Stokes equation: [22]

$$\frac{\partial}{\partial t}(\rho_f \vec{v}) + \nabla.(\rho_f \vec{v}\vec{v}) = -\nabla.P + \nabla.(\bar{\bar{\tau}}) + \rho_f \vec{g} + \vec{F} \quad (2)$$

where:

P is the static pressure

$\vec{g}$ is gravitational force vector

$\vec{F}$ is the body force vector

$\bar{\bar{\tau}}$ is defined as:

$$\bar{\bar{\tau}} = \mu[(\nabla\vec{v} + \nabla\vec{v}^T)] - \frac{2}{3}\nabla.\vec{v}I \quad (3)$$

where:

μ is the lubricant viscosity

I is the identity matrix

Energy Equation

The following energy equation was used to evaluate the temperature across the oil film of the bearing [25]

$$\rho_f C_p \left(u.\frac{\partial T}{\partial x} + w.\frac{\partial T}{\partial z}\right) = \frac{\partial}{\partial y}\left(k\frac{\partial T}{\partial y}\right) + \mu\left[\left(\frac{\partial u}{\partial y}\right)^2 + \left(\frac{\partial w}{\partial y}\right)^2\right] \quad (4)$$

where:

k is the thermal conductivity of the lubricant

C_p is the specific heat of the oil $J/kg\ °C$

The steady-state performance of the journal bearing can be performed by turning off the $\partial/\partial t$ terms.

Cavitation model

The mass transfer can be obtained using the following vapor transport equation [31]:

$$\frac{\partial}{\partial t}(a_v.\rho_v) + \nabla(a_v.\rho_v.v_v) = (R_e - R_c) \quad (5)$$

The growth of a single bubble growth is governed by the following equation:

$$R_b.\frac{d^2R_b}{dt^2} + \frac{3}{2}\left(\frac{dR_b}{dt}\right)^2 = \frac{p_v - p}{\rho_f} - \frac{2\sigma}{\rho_f R_b} - \frac{4\mu}{\rho_f.R_b}.\frac{dR_b}{dt} \quad (6)$$

where:

R_b is the bubble radius

σ is the surface tension

p is the static pressure

p_v is the vapor pressure

Equation (6) is simplified by Neglecting the second order terms and the surface tension as follows:

$$\frac{dR_b}{dt} = \sqrt{\frac{2}{3}.\frac{p_v - p}{\rho_f}} \quad (7)$$

Zwart-Gerber-Balamri model is adopted in the present work. It assumes the same bubble size in the system. The final form of this cavitation model is as follows [31]:

If, $p < p_v$

$$R_e = F_{evap}.\frac{3.a_{nue}(1-a_v).\rho_v}{R_b}.\sqrt{\frac{2}{3}.\frac{p_v - p}{\rho_f}} \quad (8)$$

If, $p \geq p_v$

$$R_c = F_{cond}\frac{3.a_v.\rho_v}{R_b}.\sqrt{\frac{2}{3}.\frac{p - p_v}{\rho_f}} \quad (9)$$

where:[31]

R_b bubble radius. It was taken as 10^{-6} m.

a_{nue} nucleation site volume fraction. It was taken as 5×10^{-4}.

F_{evap} evaporation coefficient. It was taken as 50

F_{cond} condensation coefficient. It was taken as 0.01.

2.3 Thermal and Rheological Properties of the lubricant

In the present work the lubricant viscosity was assumed to be a function of temperature and the volume fraction of the nanoparticles. The modified Krieger Dougherty model implemented with Barus-law was used to evaluate the nano- lubricant viscosity as a function of the nanoparticles volume fraction and the oil film temperature [26].

$$\mu = \mu_o exp[-\beta(T - T_{in})]\left(-\frac{\varphi_a}{\varphi_m}\right)^{-2.5\varphi_m} \quad (10)$$

where:

$$\varphi_a = \varphi\left(\frac{a_a}{a}\right)^{3-D}$$

μ is the dynamic viscosity of the nano lubricant ($N.s/m^2$)

μ_0 is the dynamic viscosity of the base oil at the inlet temperature.

φ is the volume fraction of the nanoparticles.

$\frac{a_a}{a}$ aggregate ratio

D represents the fractal index for Nano fluids with a standard value of 1.8 [27].

The experimental results of the viscosity for the base oil SAE40W (produced by al dura refinery-Iraq) blended with 13 nm TiO_2 nanoparticles published by Asmaa et al. [24] have been used to determine the value of the effective radius of the nanoparticles aggregate required for the application of Krieger-Dougherty viscosity model. The procedure of Kole and Dey [28] was followed in the present work to evaluate the required aggregate ratio of such nano-lubricant. The information of the oil viscosity was compared with that obtained by the Krieger-Dougherty equation which is a function of nanoparticles volume fraction for various possible aggregate ratios. It was found that all the experimental data of the viscosity located between the predicted curves for values of aggregate ratios ranging from 3 to 4. Fairly good agreement was obtained for aggregate ratio of 3.3 which is close to that obtained by Gundarneeya [16] taking into consideration the different types of the base oil used in both studies. The experimental values of the lubricant viscosities [24] are compared with that predicted by Krieger-Dougherty equation with aggregate ratio mentioned above is depicted in Fig. 2. This figure clearly shows the good agreement between the predicted and the measured viscosity with 6% maximum deviation between the results for the viscosity at a temperature of 60 °C.

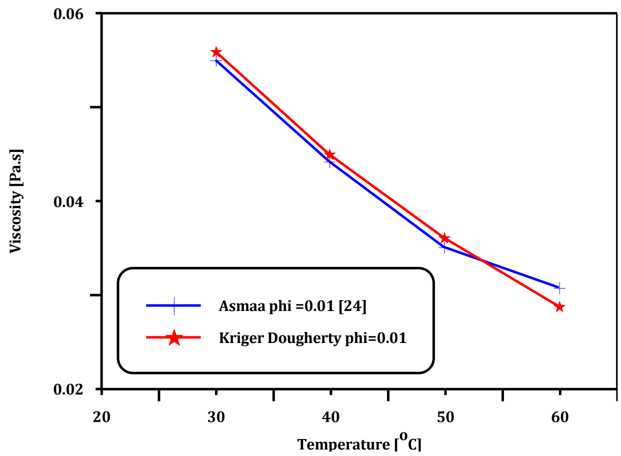

Fig. 2. TiO_2 Nano-lubricant viscosity vs. temperature.

Also, the experimental data for the thermal conductivity of such nano-lubricant has been correlated to obtain the thermal conductivity as a function of temperature. The following empirical equation was obtained using IBM SPSS statistica with R^2=98.07%.

$$k_{fT} = k\ e^{[4.1*10^{-3}(T-303))]} \tag{11}$$

where:

k_{fT} is the pure oil thermal conductivity (W/m^2. K)

T is the Nano-lubricant temperature in Kalvin.

Equation (9) was implemented with the Maxwell-Garnett's model to obtain the thermal conductivity for the nano lubricant as a function of temperature and nanoparticles volume fraction as follows:

$$k_{nf} = k_{fT}\left[\frac{(k_p+2k_{fT})-2\varphi(k_{fT}-k_p)}{(k_p+2k_{fT})+\varphi(k_{fT}-k_p)}\right] \tag{12}$$

Fig. 3 shows a comparison between the values of SAE40W/TiO_2 nano-lubricant thermal conduc-tivity calculated by using equation (12) and that published by [24]. The maximum deviation between the results was calculated and found to be 9.4% at 60^{o}C.

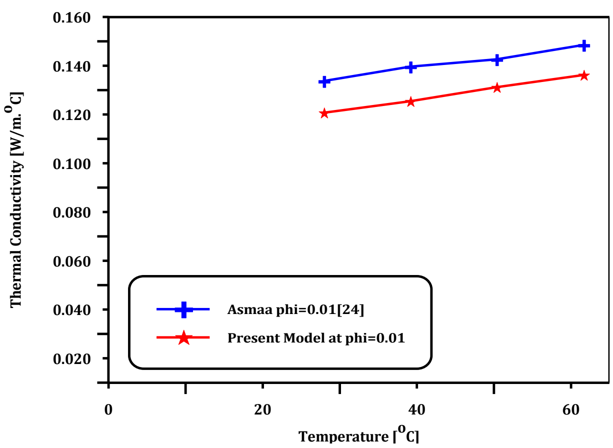

Fig. 3. Thermal conductivity Vs. temperature,

The density of the Nanolubricant can be evaluated as cited in [25]

$$\rho_{nf} = (1-\varphi)\rho_f + \varphi\rho_p \tag{13}$$

The specific heat of the nano-lubricant can be evaluated as cited in [25]:

$$\rho_{nf}C_{pnf} = (1-\varphi)(\rho C_p)_f + \varphi(\rho C_p)_p \tag{14}$$

2.4. Deformation Calculation

The following two-dimensional deformation model is used to obtain elastic deformation of the bearing material.

$$[K_p]\{\delta\} = \{F\} \tag{15}$$

where:

$\{F\}$ is the force vector which was calculated from the nodal oil film pressure

$[K_p]$ is the global stiffness matrix.

$\{\delta\}$ is the nodal displacement vector.

2.5. Performance Parameters

The load components in x and y directions can be evaluated as [29]:

$$F_x = \iint_{A_j} P_j \cdot \sin\theta \tag{16}$$

$$F_y = \iint_{A_i} P_j \cdot \cos\theta \cdot (dA_j) \tag{17}$$

The total load carried by the bearing can be evaluated as:

$$W = \sqrt{(F_x)^2 + (F_x)^2} \tag{18}$$

The attitude angle can be calculated as [29]:

$$\phi = \tan^{-1}\left(\frac{F_y}{F_x}\right) \tag{19}$$

The friction force at the bearing and the journal surfaces can be evaluated as[29]:

$$F_{fr} = \iint \tau \cdot dA \tag{20}$$

Hence, the friction coefficient can be calculated as:

$$f = \frac{F_{fr}}{W} \tag{21}$$

The oil side leakage flow can be expressed as[29]:

$$Q_s = \int_{\theta_1}^{\theta_2} \frac{h^3}{12\mu}\left(\frac{\partial P}{\partial z}\right)_{z=0 and\ L} d\theta \tag{22}$$

where h is the oil film thickness which can be expressed as:

$$h = C \cdot (1 - X \cdot \cos\theta - Y \cdot \sin\theta) \tag{23}$$

Taking into consideration the elastic and thermal deformations of the bearing material the modified oil film thickness can be written as:

$$h = C.(1 - X \cdot \cos\theta - Y \cdot \sin\theta + \delta_E + \delta_T) \quad (24)$$

where

δ_E *and* δ_T are the elastic and thermal deformations of the bearing material respectively.

2.6. Boundary conditions

The discretized model of the journal bearing of the present work is shown in Fig 4. The lubricant was assumed Newtonian in laminar flow condition. The bearing surfaces are assumed to be smooth. The inlet pressure was assumed (0.2 MPa), while the outlet pressure is atmospheric. The bearing assumed to consist of stationary bearing interface and rotating wall journal with rotational speed (2000-4000 rpm). The thermal boundary conditions include the inlet oil temperature (40 °C), the outlet temperature and convection heat transfer from the outside surface of the bearing. The following conditions must be satisfied at the interaction surface [30]:

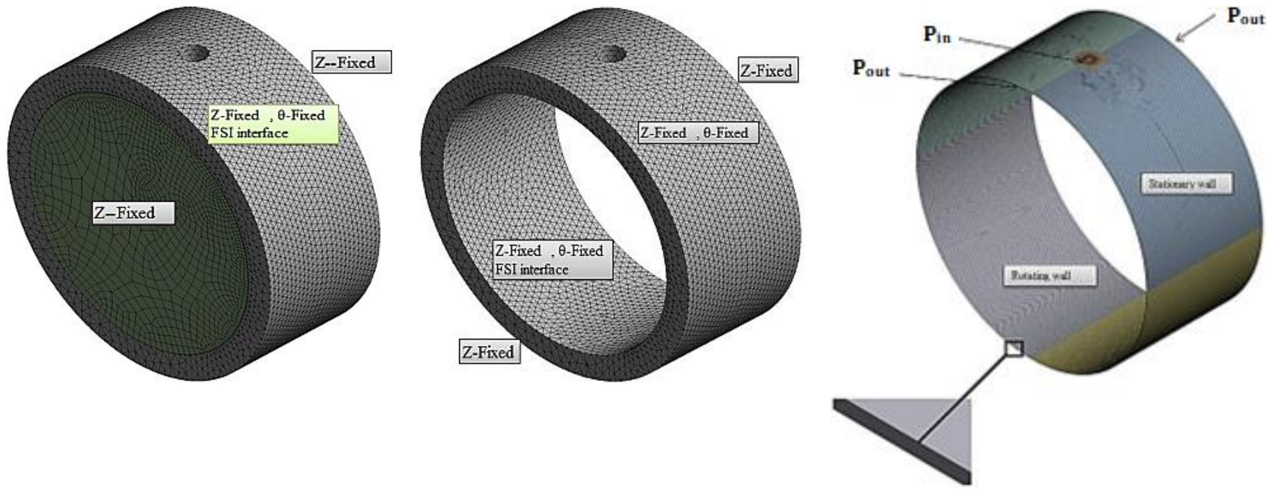

Fig. 4. Fluid and solid Domains (a) shaft (b) bearing (c) fluid domain.

Continuity of pressure

$$p_f . n_f = p_s . n_s$$

Continuity of displacement

$$\delta_f = \delta_s$$

Continuity of heat flux

$$q_f = q_s$$

Continuity of temperature

$$T_f = T_s$$

where f and s denoted for fluid and solid respectively.

3. METHOD OF SOLUTION AND VALIDATION

The fluid field velocities and temperature were calculated using FLUENT software. Zwart-Gerber-Belamari model [31], was used to consider the cavitation effect. The pressure-velocity coupling was solved iteratively using SIMPLE algorithm. A first order upwind scheme was used for momentum and energy equations while PRESTO and QUICK were used for pressure and volume fraction. To ensure the accuracy of the solution, a mesh independence study for the Thermoelstohydrodynamic (TEHD) model was conducted for a journal bearing working at an eccentricity ratio of 0.5 and a rotating speed of 1000 rpm. It was performed by observing the predicted pressure, deformation, and the load for various levels of grid refinements as illustrated in table (2). It was observed that using hexahedral element with thickness of 0.3mm, three layers in the radial direction and total number of 133767 in circumferential direction leads to a good mesh quality with an aspect ratio of 35.966 as highlighted by the yellow color in the table. The solid domain was also discretized into 86871 tetrahedral finite elements in the circumferential direction to evaluate the material deformation. The two-way FSI model was used for more accurate calculation of the elastic deformation of the bearing material. The TEHD model of the present work was validated by comparing the oil film pressure and the bearing material deformation contours obtained in the present work with those obtained by Dhande [29]as presented in Fig. 5a to Fig. 5d. These figures show that the findings demonstrate a high degree of agreement with a deviation of about 4% and 2% between the results of the pressure and the deformation respectively. The red contours show that the location of the maximum pressure and deformation are the same in both works. Another validation was performed by comparing the pressure obtained in the present work (blue solid curve) with that obtained numerically by Li etal [32](red triangles) and experimentally by Ferron and Boncompain [33](black squares) as illustr-ated in Fig. 6. The results of the present work agreed well with that obtained by Li et al. and reasonably with the experemental results obtained by Ferron and Boncompain with maxi-mum deviation of 2% between the results.

Table 2. results of fluid and solid domains for various mesh grid densities

Body Size (mm)	Mesh layers (r)	Aspect ratio	Element number	Pressure (Pa)	Deformation (μm)	Load (N)
0.9	3	107.13	15366	655794.6	0.030743	360.7267152
0.8	3	94.225	19509	655321.6	0.030753	360.1868488
0.7	3	83.326	25116	646503.7	0.030319	356.5371553
0.6	3	71.422	33996	657520.7	0.030898	360.8967868
0.5	3	59.995	48042	657881.6	0.030921	359.1397649
0.4	3	47.615	76185	657572.6	0.030925	351.7762836
0.3	3	35.966	133767	657762.3	0.030932	343.2067273
0.2	3	23.998	298956	657755.8	0.030938	338.8426399

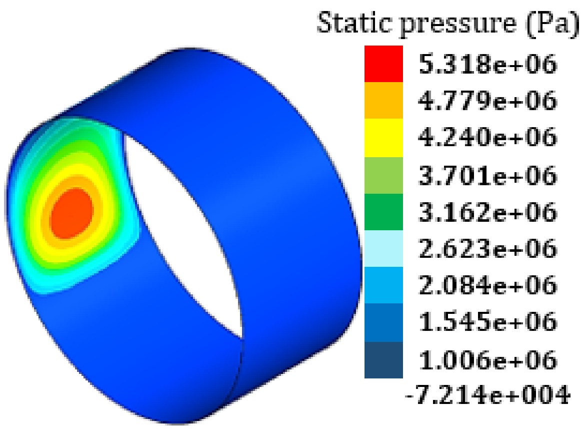

(a)

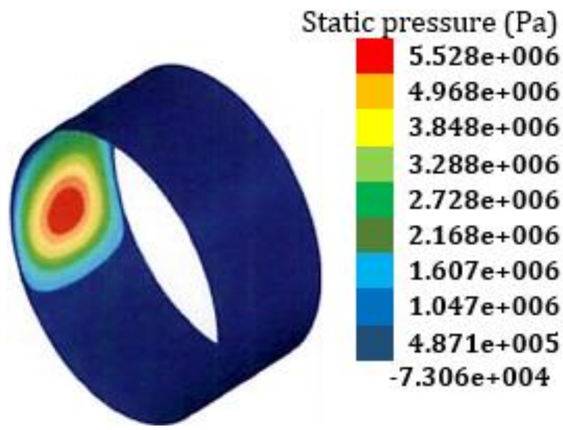

(b)

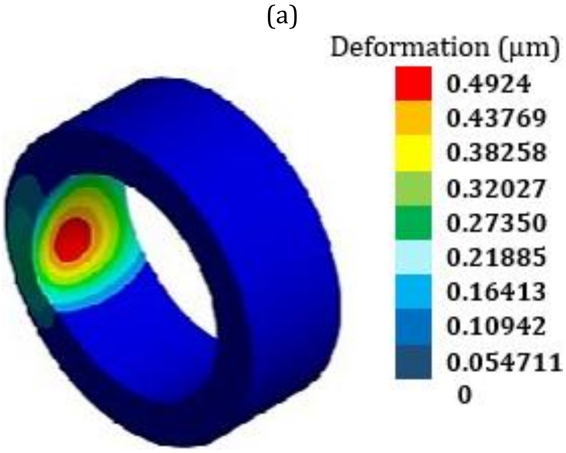

(c)

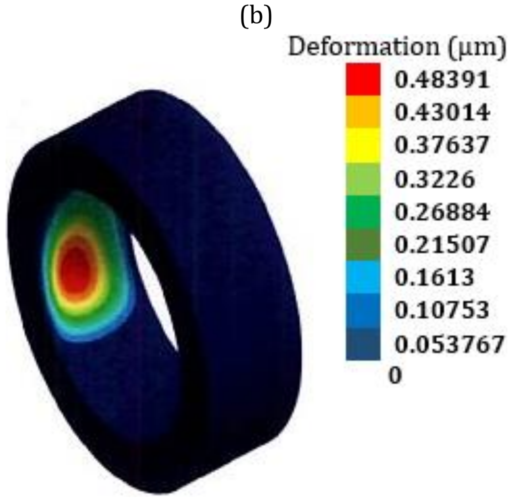

(d)

Fig. 5. (a, b) Pressure contour (c, d) Deformation contour of the present work and Dhande and Yashwant [29].

4. RESULTS AND DISCUSSION

The effect of TiO_2 nano-lubricant with different volume fractions of the nanoparticles on the performance of the journal bearing working at different journal speeds and eccentricity ratios will be presented and discussed in this section.

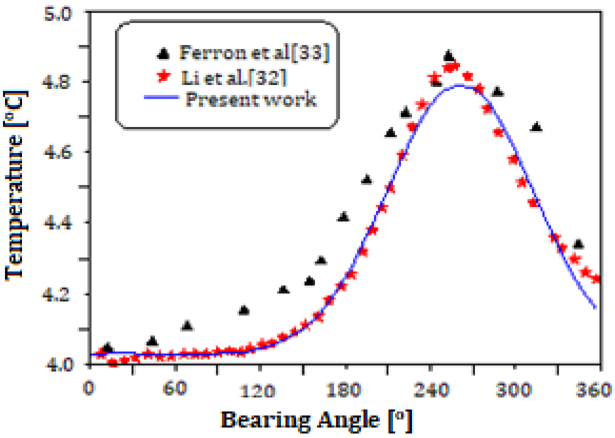

Fig. 6. Pressure of the present work compared to the experimentally obtained by Ferron and Boncompain and numerically by Li et al.

Fig. 7a and Fig. 7b show the pressure contours when the bearing lubricated with pure oil and that dispersed by 1.5% TiO_2. It has been noticed the oil film pressure increases from 1.37 MPa to 1.95 MPa with percentage increase of 12.7% when the bearing lubricated by the nanolubricant rather than pure oil as indicated by the red color of the contours. This can be attributed to the increase in the lubricant viscosity of the nano-lubricant. The maximum pressure located at the minimum gap region. However, the increase in oil film pressure has been obtained without an increase in the oil film temperature as can be observed from Fig. 8a and Fig. 8b. with a uniform temperature distribution across the oil film.

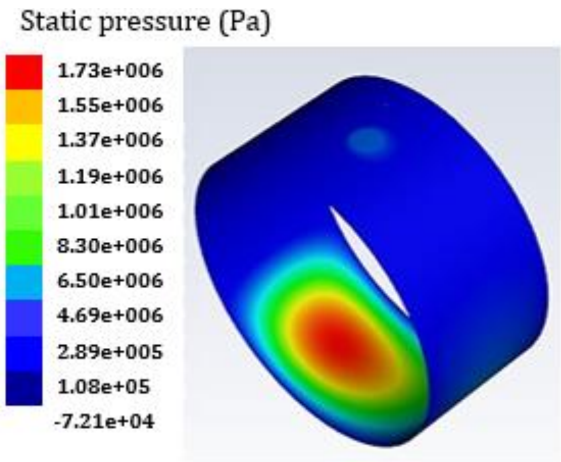

(a)

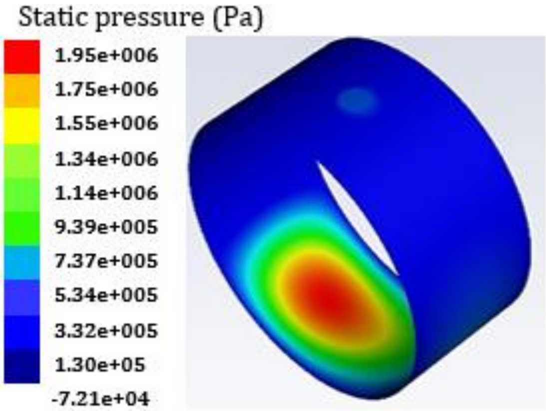

(b)

Fig. 7. Pressure distribution (a) pure oil (b) nano-lubricant, ε=0.6.

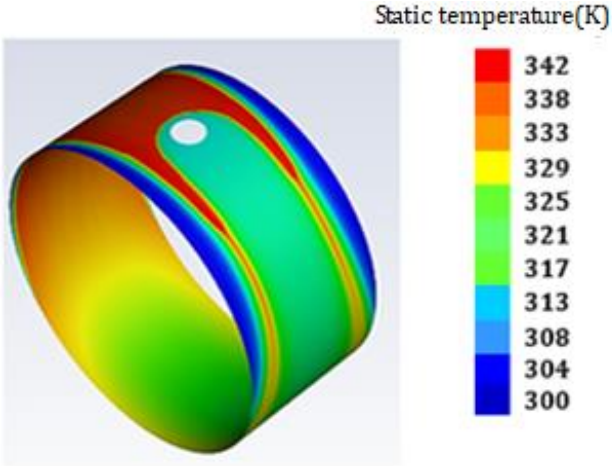

(a)

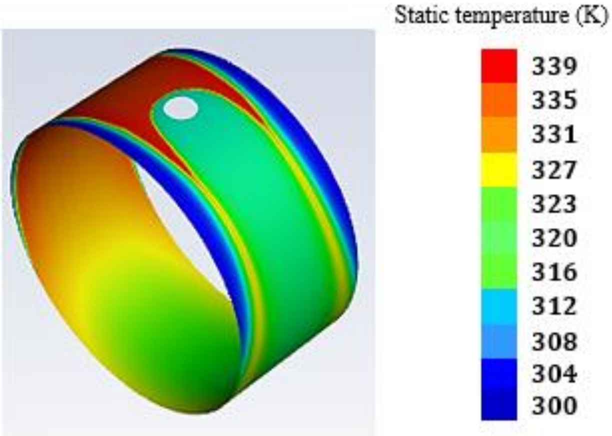

(b)

Fig. 8. Temperature distribution (a) pure oil (b) nano-lubricant.

Fig. 9a and Fig. 9b show the vapor volume fraction when the bearing lubricated with pure oil and 1.5% TiO_2 nano-lubricant. It was observed that the bearing shows nearly the same vapor volume fraction when it was lubricated with nano-lubricant and pure oil.

The maximum values reach 9.44×10^{-1} and 9.45×10^{-1} as indicated by the red contours when it was lubricated with pure and nano-lubricant. How-ever, the area of the cavitation zone seems to be smaller for the bearing lubricated with nano-lubricant.

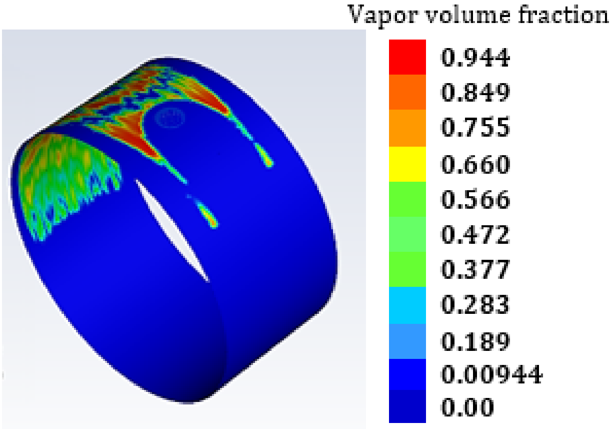

(a)

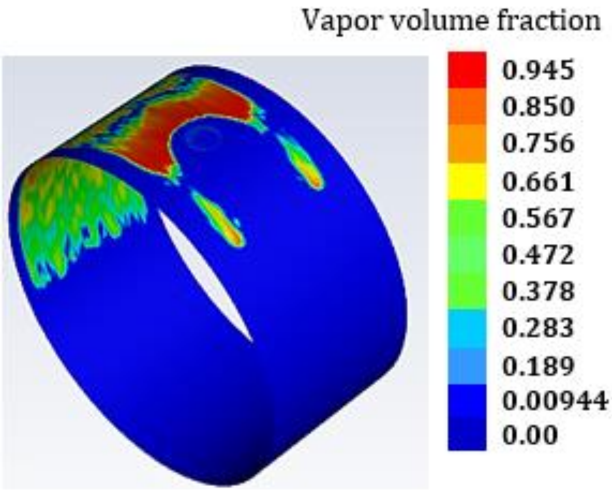

(b)

Fig. 9. Vapor volume fraction (a) pure oil (b) nano-lubricant, ε=0.6.

Fig. 10 illustrates a comparison between the distribution of the circumferential pressure when the bearing lubricated with pure oil and nano-lubricant. It can be pointed that the peak pressure dropped by about 17% and 50% when the cavitation was taken into consideration for the bearing lubricated with pure and 1.5% TiO_2. nano-lubricant with a decrease in cavitation zone size when using nano-lubricant. This can be explained by the decrease in the density and lubricant viscosity of the lubricant at the cavitation zone. The results obtained was supported by that obtained in [31].

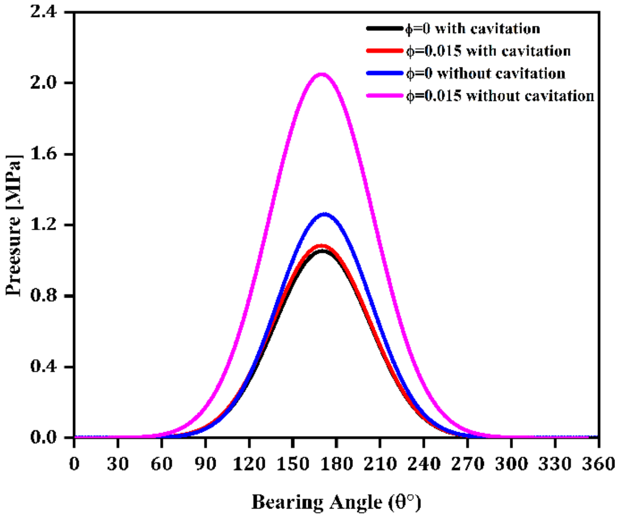

Fig. 10. Comparison of the pressures distribution in journal bearing with and without cavitation. L/D=0.5.

Fig. 11 shows the maximum oil film pressure when the bearing works at different eccentricity ratios and lubricated with oil containing different TiO_2 nanoparticles. It depicts that the bearing maxim-um pressure became higher when it works at higher eccentricity ratio as a result of the thinner oil film in this case. The increase becomes more noticeable when the bearing lubricated with nano-lubricant that has higher particle concentration. It was observed that the maximum pressure increases by about 16% and 29% when the bearing works at eccentricity ratios of 0.8 and 0.9 respectively when it was lubricated with 1.5%TiO_2 nano-lubricant. This can be assigned to the higher viscosity of the nano lubricant.

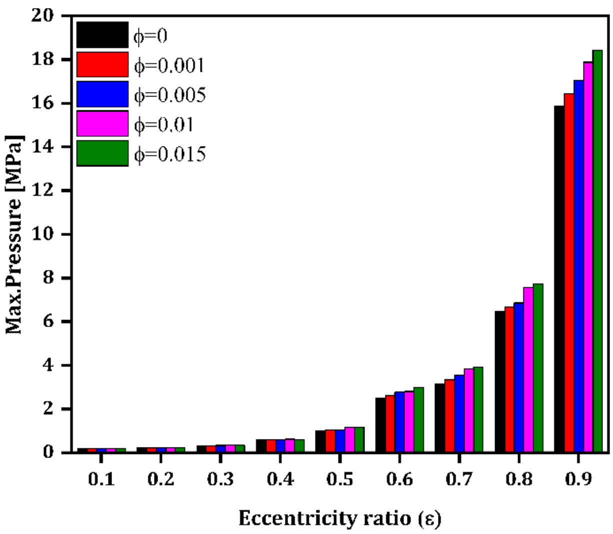

Fig. 11. Maximum pressure vs. eccentricity ratio.

Fig. 12 illustrates the increase in the maximum oil film pressure with the journal speed especially when it was lubricated with nano-lubricant that has higher particle concentration of the TiO_2 nanoparticles due to the higher viscosity of the lubricant in this case.

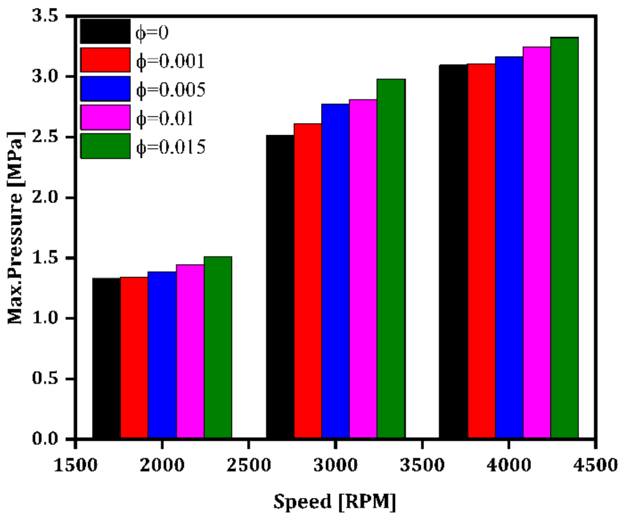

Fig.12. maximum oil film pressure vs. journal speed

Fig. 13 illustrates an increase in the load carried by the bearing when it was lubricated with nano-lubricant that has higher volume fractions of the nanoparticles as a result of the higher oil film pressure generated in this case especially when it works at higher eccentricity ratios. It can be also observed that nano lubricant has a little effect on the load carried by the bearing when it works with smaller eccentricity ratios ($\varepsilon \leq 0.4$) since the lubricant behaves as pure oil when a little amount of the nanoparticles was dispersed in the base oil.

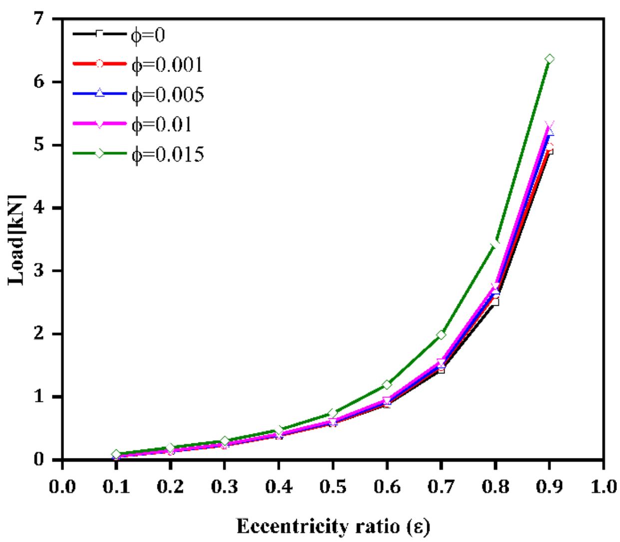

Fig. 13. Load carrying capacity vs eccentricity ratio

The effect of TiO_2 nanoparticles volume fraction on the circumferential oil film temperature distribution when the bearing works at an eccentricity ratio of 0.6 and journal speed of 3000 rpm is illustrated in Fig. 14. It was observed that the oil film temperature increases by 15% as the bearing lubricated with 1.5%volume fraction of TiO_2 nano lubricant compared with that lubricated with pure oil. This can be explained by the higher viscosity of the nano-lubricant which causes in a higher shear stress of the lubricant. This figure also depicts that the maximum oil film temperature slightly increased when smaller volume fraction of the nanoparticles was dispersed in the base oil.

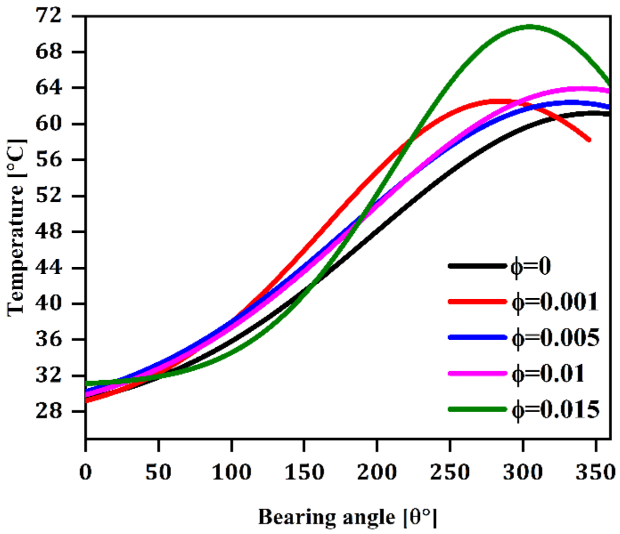

Fig. 14. Circumferential oil film temperature, $\boldsymbol{\varepsilon}$ =0.5, N=3000rpm.

It becomes higher when the bearing works at higher eccentricity ratios as a result of thinner oil film and higher friction force as can be shown in Fig. 15. This figure depicts that the friction force at the bearing surfaces increases by 38.7% when the bearing works at 0.9 eccentricity ratio and lubricated with 1.5% TiO_2 nano-lubricant in comparison with that lubricated with pure oil. This figure also shows that the existence of the nanoparticles with small amounts ($\phi < 1.5\%$) in the base oil has a little effect on the friction force. However, Fig. 16 shows that using the nano lubricant with different nanoparticles volume fractions have a little effect on the coefficient of friction. Fig. 17 shows that the maximum oil film temperature slightly increases with the journal speed. It becomes higher when higher nanoparticles concentration of TiO_2 dispersed in the base oil due to the increase in the induced friction force.

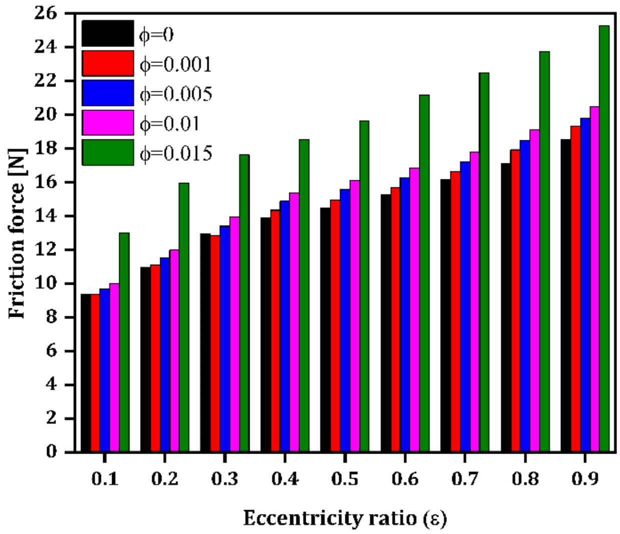

Fig. 15. Maximum friction force vs. eccentricity ratio.

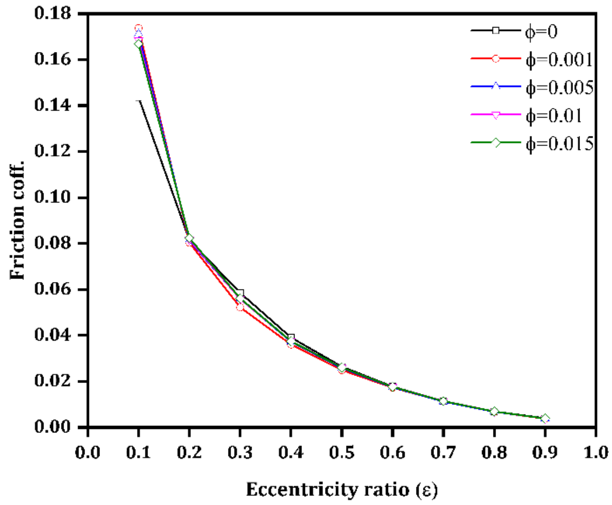

Fig. 16. friction coefficient vs. eccentricity ratio.

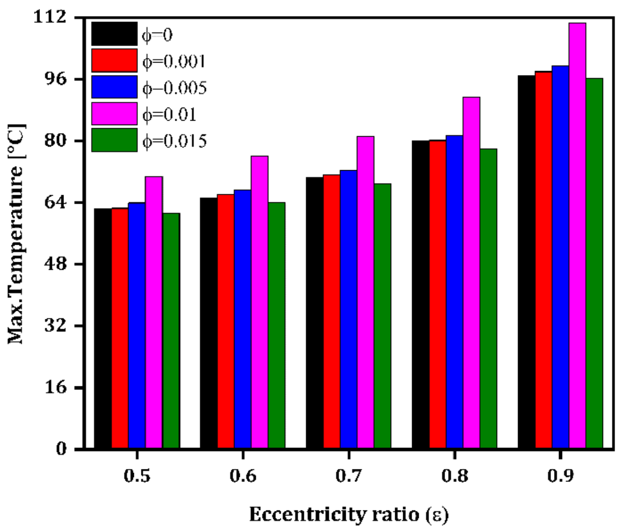

Fig. 17. Maximum oil film temperature vs. journal speed.

Fig. 18 shows that bearing lubricated with the nano-lubricant has a lower oil side leakage flow. This can be attributed to the higher viscosity of the lubricant which decreases it velocity in axial direction. The flow of oil becomes higher as the bearing works at higher eccentricity ratio due to the increase in the oil film pressure.

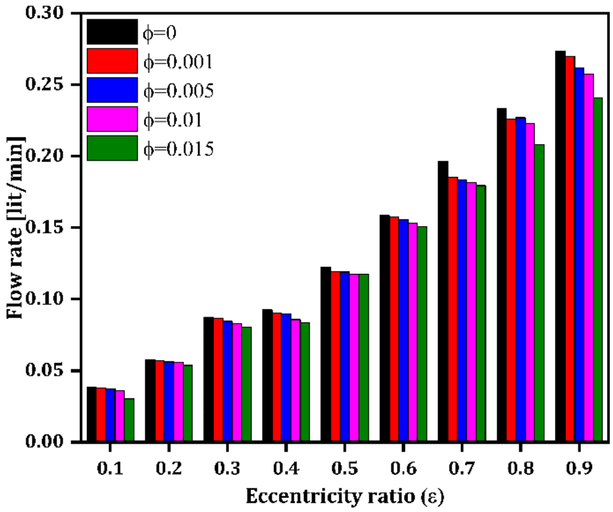

Fig. 18. flow rate vs eccentricity ratio.

Fig. 19 shows that the attitude angle decreases when the bearing lubricated with nano lubricant. The higher the particle concentration the higher the decrease in the attitude angle. The decrease in attitude angle becomes higher when the bearing works at higher eccentricity ratios. This can be explained by the increase of the load components in this case.

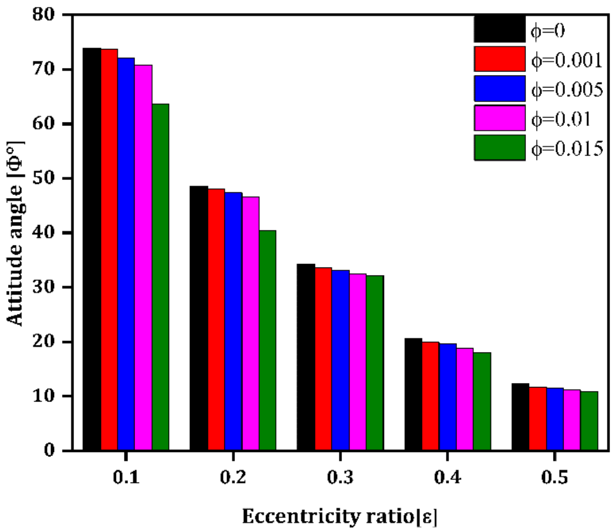

Fig. 19. Attitude angle vs. eccentricity ratio.

The bearing material deformation increases when the bearing lubricated with TiO_2 nano-lubricant as can be shown in Fig. 20. The increase in deformation becomes higher when the bearing works at higher eccentricity ratio and lubricated with nano lubricant that has higher volume fraction of TiO_2 nanoparticles due to the higher oil film pressure generated under these circumstances.

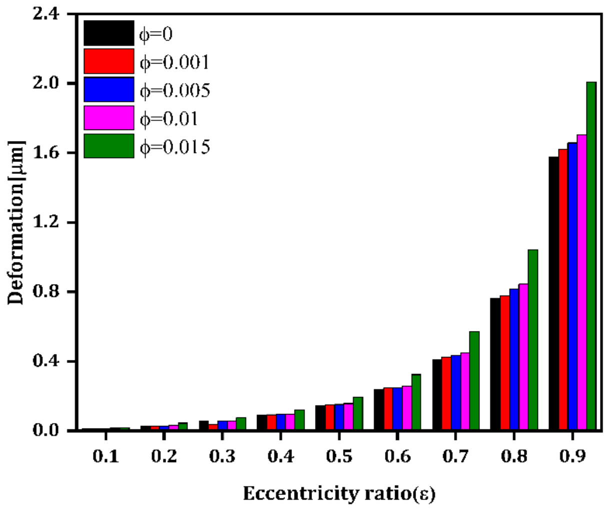

Fig. 20. deformation vs. eccentricity ratio.

Fig. 21 shows that the bearing material deformation increases as the bearing works at higher journal speeds mainly when it was lubricated with oil dispersed with higher percentage of the nanoparticles. This can be attributed to the higher oil film pressure generated in this case.

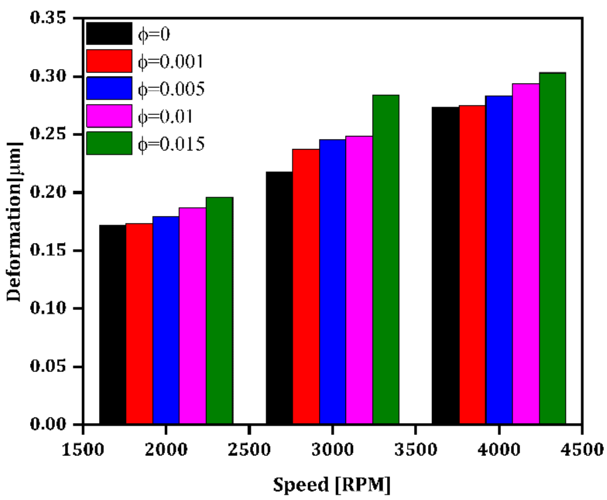

Fig. 21. deformation vs journal speed

The effect of considering the elastic deformation of the bearing material on the oil film pressure can be seen in Fig. 22. It was observed that the maximum oil film pressure decreases due to the effect of the elastic deformation of the bearing material which increases the oil film thickness in this case and in turn affects the bearing performance parameters of the bearing.

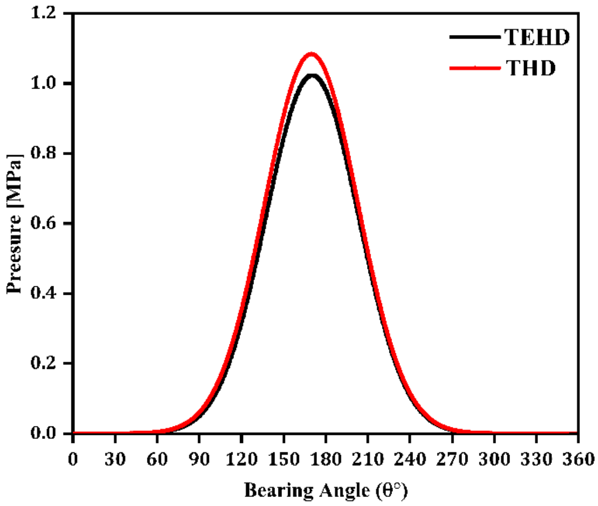

Fig. 22. circumferential oil film pressure under TEHD and THD conditions. (L/D=0.5)

5. SHAFT EQUILIBRIUM POSITION

The shaft's equilibrium position can be determined by fixing the shaft rotational axis at a prelimited position concerning attitude angle and eccentricity in a parametric form. The effect of the bearing material elastic deformation was studied by transforming the fluid forces obtained by using CFD technique to the structural domain and vice-versa. Equilibrium position is then determined by using the design optimization. Design of experiments (DOE), Response Surface Analysis (RSA), and the Optimization are the three stages followed to implement the design exploration. The design of experiment used to calculate the set of eccentricities and attitude angles required to construct the response surface in Fig. 23. This figure shows the shaft position vs. f_x, whereas Fig. 24 displays the shaft position versus f_y for 1%TiO_2 nano-lubricated journal bearing working at journal speed of 3000 rpm. Table 3 shows the DOE used to calculate a set of eccentricities and attitude angles that are used to construct the response surfaces. The eccentricity and attitude angle higher and lower bounds are stated, and the solution is expected to fall within these bounds. To obtain design points, an optimal space-filling design procedure is applied, and a matrix of experiments is created. These design features serve to create a surface that analyzes the interaction between eccentricity, angle of attitude, and output parameters (fluid reaction forces).

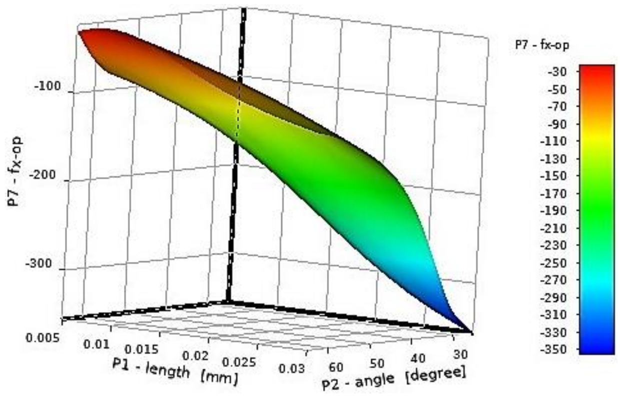

Fig. 23. Shaft location in terms of eccentricity vs.f_x .

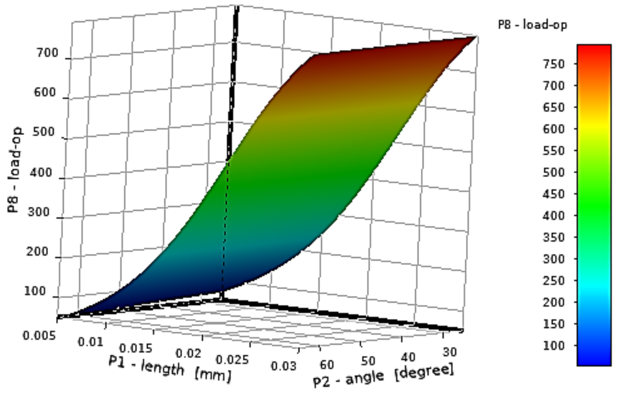

Fig. 24. Response surface for vertical load.

Table 3. Design points.

	A	B	C	D	E	F	G	H	N	O	P
1	Name	Update order	P1-Length (mm)	P2-angle (degree)	P3-Mesh Max	P6-fy-op.	P7-fx-op.	P8-Load op.	P14-X Origin (m)	P15-Y Origin (m)	P16-ecc. ratio
2	1 OP7	7	0.02305	31.667	33.370	-397.1	-273.75	482.32	-1.21E-05	-1.962E-05	0.46111
3	2 OP9	9	0.02661	45.556	42.039	-738.3	-205.83	266.54	-1.86E-05	-2.173E-05	0.57222
4	3 OP3	3	0.01194	53.889	30.291	-125.6	-97.144	158.86	-9.64E-05	-7.039E-06	0.23339
5	4 OP6	6	0.02027	43.444	32.077	-348.3	-132.74	372.74	-1.54E-05	-1.318E-05	0.40556
6	5 OP2	2	0.00916	27.222	27.585	-40.56	-132.38	138.45	-4.19E-05	-8.151E-06	0.18333
7	6 OP4	4	0.01472	36.111	28.399	-150.2	-121.12	227.20	-6.62E-05	-1.189E-06	0.29444
8	7 OP5	5	0.0175	62.778	34.030	-264.4	-65.547	272.48	-1.55E-05	-3.005E-06	0.35000
9	8 OP8	8	0.02583	58.333	37.205	-998.8	-5.4022	596.06	-2.19E-05	-1.356E-05	0.51667
10	9 OP1	1	0.00628	45.000	29.357	-31.51	-76.606	82.815	-4.51E-05	-4.517E-06	0.12778

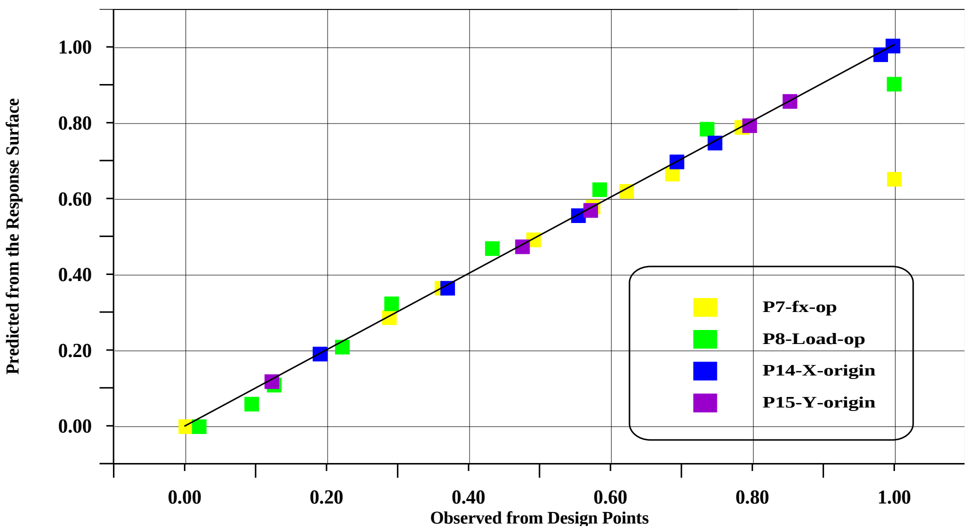

Fig. 25. Goodness of fit.

Fig. 25 shows the goodness of fit used to determine how well the surface fits the data points. The response surfaces are analyzed to determine the values of potential solutions that meet the optimization requirements. The optimization is based on the evaluation of the response surface using the Multi-Objective Genetic Algorithm (MOGA) based on notions of elitism with non-parametric analytical regression. It allows for many objectives and restrictions to be met to discover the globally optimal solution. More refinement design points are added to the solution to acquire a closer solution, and the procedure is continued until the optimum equilibrium position of the shaft is attained. Based on the restrictions given, the module provides three optimal solutions, known as candidate points in table 4. This figure indicates that the bearing has an optimum eccentricity, attitude angle, horizontal and vertical load components of 0.022 mm, 62.8^{o}, 84.456 N and 509.74 N respectively.

Table 4. Constraints on optimization and possible solutions provided by the optimization module.

Table of Schemax E4: Optimization					
	A	**B**	**C**	**D**	**E**
1	**Name**	**Parameter**	**Objective**		
2			Type	Target	Type
3	Seek P8=550	P8-load-op	Seek Target	550	No Constraint
4	Seek P7=0	P7-fx-op	Seek Target	0	No Constraint
Candidate Points					
		Candidate Point1	**Candidate Point2**	**Candidate Point3**	
P1-length(mm)		0.023006	0.023125	0.022058	
P2-angle(degree)		57.968	61.031	62.8	
P7-fx-op		★ -91.518	★★ -89.729	★★ -84.545	
P8-load-op		★★★ 550.63	★★★ 555.99	★★★ 509.74	

6. CONCLUSIONS

Full 3D CFD two-way FSI elastohydrodynamic lubrication model of journal bearing lubricated with TiO_2 nano-lubricant was demonstrated in the present work, considering thermal and cavitation effects. The simulation results are well validated with those obtained by Dhande [29] and Li et al [32]. The following concluding remarks can be drawn:

1. An increase in the oil film pressure by 12.7% was observed when the bearing lubricated by 1.5% TiO_2 nano-lubricant.
2. The maximum oil film temperature slightly increased when smaller volume fraction of the nanoparticles were dispersed in the base oil. it becomes higher when the bearing works at higher eccentricity ratios as a result of thinner oil film and higher friction force.
3. A decrease in oil side leakage flow was observed when the bearing lubricated with nano-lubricant.
4. Cavitation has a significant effect on the performance of journal bearing. The maximum oil film pressure decreases by 17% when the bearing lubricated with nano-lubricant and considering the cavitation effect. It can not be neglected for proper analysis.
5. The elastic deformation of the bearing material has a significant effect on its performance. It must be considered and cannot be neglected for proper analysis. The maximum oil film pressure decreases when the elastic deformation was considered.
6. An increase in the bearing material deformation was observed with the journal speed. It was become significant at higher speeds and cannot be neglected.
7. The maximum pressure increaese when the bearing works at higher rotational speed and eccentricity ratios.
8. The location of the journal center, the optimum value of the load carried by the bearing and the attitude angle were sucessfully obtained using Multi-Objective Genetic Algorithm (MOGA).
9. The cavitation zone size was decreased for the bearing lubricated with nano-lubricant.

Appendix -A-
User-Defined Function (UDF) for specifying a temperature-dependent viscosity

```
include "udf.h"
#define BETA 0.034
#define Tin 313
#define muin 0.0985
DEFINE_PROPERTY(cell_viscosity, cell, thread)
{
real mu_lam;
real temp=C_T(cell, thread);
mu_lam=muin*exp(-BETA*(temp-Tin));
return mu_lam;
}
```

REFERENCES

[1] N. K. Prabhakaran, P. K. R. Kumar, and K. S. Babu, "Thermohydrodynamic analysis of journal bearing operating under nanolubrica-nts," *Proceedings of the ASME/ STLE Interna-tional Joint Tribology Conference IJTC*, pp. 17-21, Sep. 2011, doi:10.1115/IJTC2011-61244.

[2] S. B. Kalakada, P. N. Kumarapillai, and R. K. P. K, "Static characteristics of thermohydrodynamic journal bearing operating under lubricants containing nanoparticles," *Industrial Lubrication and Tribology*, vol. 67, no. 1, pp. 38–46, Feb. 2015, doi: 10.1108/ilt-01-2013-0015.

[3] K. G. Binu, B. Shenoy, D. S. Rao, and R. Pai, "Static characteristics of a fluid film bearing with TiO_2 based nanolubricant using the modified Krieger–Dougherty viscosity model and couple stress model," *Tribology International*, vol. 75, pp. 69–79, Jul. 2014, doi: 10.1016/j.triboint.2014.03.013.

[4] A. Singh, N. Verma, A. Chaurasia, and A. Kumar, "Effect of TiO_2 additive volume fraction in lubricant oil on the performance of hydrodynamic journal bearing," *IOP Conference Series*, vol. 802, no. 1, p. 012005, Mar. 2020, doi: 10.1088/1757-899x/802/1/012005.

[5] V. B. Awati and A. Kengangutti, "Static Characteristics of Thermohydrodynamic Journal Bearing with Surface Roughness Operating Under Lubricants with Nanoparticles," *Journal of Nanofluids*, vol. 7, no. 1, pp. 203–209, Feb. 2018, doi: 10.1166/jon.2018.1429.

[6] K. R. Yathish, K. G. Binu, B. Shenoy, D. S. Rao, and R. Pai, "Study of TIO_2 nanoparticles as lubricant additive in Two-Axial Groove Journal Bearing," *Zenodo (CERN European Organization for Nuclear Research)*, Oct. 2014, doi: 10.5281/zenodo.1096705.

[7] A. Kumar, S. K. Kakoty, "A variable viscosity approach for the analysis of steady state and dynamic characteristics of two-lobe journal bearing with TiO_2 based nano-lubricant," *Gas Turbine India Conference, American Society of Mechanical Engineers*, Dec. 2017, doi: 10.1115/GTINDIA2017-4646.

[8] A. Kumar and S. K. Kakoty, "Effect of couple stress parameter on steady-state and dynamic characteristics of three-lobe journal bearing operating on TiO_2 nanolubricant," *Proceedings of the Institution of Mechanical Engineers, Part J: Journal of Engineering Tribology*, vol. 234, no. 4, pp. 528–540, Jul. 2019, doi: 10.1177/1350650119866028.

[9] S. R. Suryawanshi and J. T. Pattiwar, "Effect of TiO_2 Nanoparticles Blended with Lubricating Oil on the Tribological Performance of the Journal Bearing," *Tribology in Industry*, vol. 40, no. 3, pp. 370–391, Sep. 2018, doi: 10.24874/ti.2018.40.03.04.

[10] R. Ramaganesh, S. Baskar, G. Sriram, S. Arumugam, and M. Ramachandran, "Finite element analysis of a journal bearing lubricated with nano lubricants," *FME Transactions*, vol. 48, no. 2, pp. 476–481, Jan. 2020, doi: 10.5937/fme2002476r.

[11] A. Dhanola and H. C. Garg, "Thermohydrodynamic (THD) Analysis of Journal Bearing Operating with Bio-based Nanolubricants," *Arabian Journal for Science and Engineering*, vol. 45, no. 11, pp. 9127–9144, Jun. 2020, doi: 10.1007/s13369-020-04651-y.

[12] P. Khan, A. Dhanola, and H. C. Garg, "Elasto-hydrodynamic analysis of journal bearing operating with nanolubricants," *Proceedings of the Institution of Mechanical Engineers, Part J: Journal of Engineering Tribology*, vol. 235, no. 5, pp. 963–974, Jun. 2020, doi: 10.1177/1350650120931979.

[13] K. Parthasarathy, S. Baskar, S. Arumugam, G. Prabaharan, and M. C. G. Shankar, "Fuzzy Logic Model of Journal Bearing Lubricated with Nano Lubricant," *International Journal of Vehicle Structures & Systems*, vol. 12, no. 1, Jun. 2020, doi: 10.4273/ijvss.12.1.22.

[14] S. Salunke, M. Gaikwad, "Perform-*ance Analysis of Nano-Particle Infused Lubricant in Hydrodynamic Journal Bearing*," *International Advanced Research Journal in Science, Engin-eering and Technology*, vol.,7, no.3, pp.56-60, 2020. doi 10.17148/IARJSET.2020.7308.

[15] M. Hussain, V. Gaval, and A. P. Pratap, "Study of Vegetable Oil based Biolubricants and its Hydrodynamic Journal Bearing Application: A review," *Tribology in Industry*, vol. 43, no. 4, pp. 511–523, Dec. 2021, doi: 10.24874/ti.979.10.20.02.

[16] T. P. Gundarneeya and D. P. Vakharia, "Performance analysis of journal bearing operating on nanolubricants with TiO_2, CuO and Al_2O_3 nanoparticles as lubricant additives," *Materials Today: Proceedings*, vol. 45, pp. 5624–5630, Jan. 2021, doi: 10.1016/j.matpr.2021.02.350.

[17] H. Liu, H. Xu, P. Ellison, and J. Zhang, "Application of Computational Fluid Dynamics and Fluid–Structure Interaction method to the lubrication study of a Rotor–Bearing system," *Tribology Letters*, vol. 38, no. 3, pp. 325–336, May 2010, doi: 10.1007/s11249-010-9612-6.

[18] D. Benasciutti, M. Gallina, M. Munteanu, and F. Flumian, "A numerical approach for the analysis of deformable journal bearings," *Fracture and Structural Integrity*, vol. 6, no. 21, pp. 37–45, Jun. 2012, doi: 10.3221/igf-esis.21.05.

[19] M. Wodtke, A. Olszewski, and M. Wasilczuk, "Application of the fluid–structure interaction technique for the analysis of hydrodynamic lubrication problems," *Proceedings of the Institution of Mechanical Engineers, Part J:*

Journal of Engineering Tribology, vol. 227, no. 8, pp. 888–897, Apr. 2013, doi: 10.1177/1350650113481147.

[20] A. Chauhan, A. Singla, N. Panwar, and P. Jindal, "CFD based thermo-hydrodynamic analysis of circular journal bearing," *International Journal of Advanced Mechanical Engineering*, vol.,4, no.5, pp.475-482, Jan. 2014.

[21] Y. Zhang, G. Chen, and L. Wang, "Effects of thermal and elastic deformations on lubricating properties of the textured journal bearing," *Advances in Mechanical Engineering*, vol. 11, no. 10, p. 168781401988379, Oct. 2019, doi: 10.1177/1687814019883790.

[22] C. Yu, Y. Sun, Q. He, and J. Feng, "Elastohydrodynamic Behavior Analysis of Journal Bearing using Fluid–Structure Interaction considering cavitation," *Arabian Journal for Science and Engineering*, vol. 44, no. 2, pp. 1305–1320, Aug. 2018, doi: 10.1007/s13369-018-3467-9.

[23] M.-E. Kyrkou and P. G. Nikolakopoulos, "Simulation of thermo-hydrodynamic behavior of journal bearings, lubricating with commercial oils of different performance," *Simulation Modelling Practice and Theory*, vol. 104, p. 102128, Nov. 2020, doi: 10.1016/j.simpat.2020.102128.

[24] A. H. Dhiaa, M. I. Abdulwahab, S. M. Thahab, "Investigation of Thermal Transport Properties Enhancement of Nanoparticles Suspen-sions in the Application of Nanofluids," *Ph.D thesis submitted to Chamical engineering Dept. College of engineering*, 2016.

[25] B. A. Abass, S. Y. Ahmed, Z. H. Kadhim, "CFD analysis of elastohydrodynamic of journal bearing lubric-ated with nano-lubricant," *A Thesis Submitted to the College of Engineering*, 2022.

[26] I. M. Krieger and T. J. Dougherty, "A mechanism for Non-Newtonian flow in suspensions of rigid spheres," *Transactions of the Society of Rheology*, vol. 3, no. 1, pp. 137–152, Mar. 1959, doi: 10.1122/1.548848.

[27] P. C. Mishra, S. Mukherjee, S. K. Nayak, and A. Panda, "A brief review on viscosity of nanofluids," *International Nano Letters*, vol. 4, no. 4, pp. 109–120, Oct. 2014, doi: 10.1007/s40089-014-0126-3.

[28] M. Kole and T. K. Dey, "Effect of aggregation on the viscosity of copper oxide–gear oil nanofluids," *International Journal of Thermal Sciences*, vol. 50, no. 9, pp. 1741–1747, Sep. 2011, doi: 10.1016/j.ijthermalsci.2011.03.027.

[29] D. D. Yashwant, *Analysis of hydrody-namic journal bearing with elastic bushing*, Doctoral dissertation, department of mechanical engineering college of engineering, 2017.

[30] Liming Zhai, Zhengwei Wang, Yongyao Luo, Zhongjie Li, Xin Liu, *Application of fluid-structure interaction technique for the TEHD lubrication problems of the bidirectional thrust bearings*, International Symposium on Transport Pheno-mena and Dynamics of Rotating Machinery Hawaii, Honolulu, 2016, pp.10-15,

[31] D. Y. Dhande and D. W. Pande, "Multiphase flow analysis of hydrodynamic journal bearing using CFD coupled Fluid Structure Interaction considering cavitation," *Journal of King Saud University: Engineering Sciences*, vol. 30, no. 4, pp. 345–354, Oct. 2018, doi: 10.1016/j.jksues.2016.09.001.

[32] Q. Li, S. Zhang, Y. Wang, W. Xu, and Z. Wang, "Investigations of the three-dimensional temperature field of journal bearings considering conjugate heat transfer and cavitation," *Industrial Lubrication and Tribology*, vol. 71, no. 1, pp. 109–118, Jan. 2019, doi: 10.1108/ilt-03-2018-0113.

[33] J. R. Ferron, J. Frêne, and R. Boncompain, "A study of the thermohydrodynamic performance of a plain journal bearing comparison between theory and experiments," *Journal of Lubrication Technology*, vol. 105, no. 3, pp. 422–428, Jul. 1983, doi: 10.1115/1.3254632.

NOMENCLATURE

Symbol	Definition	Unit
L/D	Length/ journal diameter	
r_s	The radius of the shaft	mm
r_o	Bearing outer radius	mm
ε	Eccentricity ratio	0.1-0.9
$\emptyset$	Attitude angle	49^o
N	Journal rotational speed	rpm
T_i	Inlet oil temperature	^oC
C	Radial clearance	Mm
β	Viscosity temperature coeffic-ient	$^oC^{-1}$
ρ_{nf}	Density of the nanolubricant	kg/m^3
ρ_f	Oil density	kg/m^3
k	Oil thermal conductivity	W/m.^{o}C
C_{pnf}	Specific heat of the nanolub-ricant	J/kg.^{o}C
P_V	Oil vapor pressure (29185)	Pa
φ	volume fraction	(0-3)%